Effect of the Processing Techniques on the Properties of Ecocomposites Based on Vegetable Oil-Derived Mater-Bi® and Wood Flour

R. Scaffaro, M. Morreale, G. Lo Re, F.P. La Mantia

Dipartimento di Ingegneria Chimica dei Processi e dei Materiali, Viale delle Scienze, Università di Palermo, Palermo 90128, Italy

Received 9 January 2009; accepted 22 May 2009
DOI 10.1002/app.30822
Published online 16 July 2009 in Wiley InterScience (www.interscience.wiley.com).

ABSTRACT: Polymer composites based on biodegradable polymers and natural-organic fillers are becoming more and more important because of their interesting properties in terms of environmental impact, manufacturing cost, and esthetic features. In particular, the use of biodegradable polymer matrices allows obtaining a full biodegradability. One of the most interesting biodegradable polymer families is the Mater-Bi® one. In this work, we investigated the processability, the influence of different processing techniques, and the influence of the filler particle size on the properties of Mater-Bi/wood flour composites. Injection molding caused a partial degradation of the macromolecular chains, whereas single-screw extrusion followed by calendering and twin-screw extrusion provoked an increase of the elastic modulus and of the viscosity. The use of wood flour led to a significant increase of the rigidity, whereas a reduction of the ductility was observed. Because of the very similar aspect ratios of the two different filler size classes, no dramatic differences in the properties were found. These results are useful in order predicting and setting up the optimum preparation and processing strategy for the production of fully biodegradable polymer composites. © 2009 Wiley Periodicals, Inc. J Appl Polym Sci 114: 2855–2863, 2009

Key words: biodegradable; composites; extrusion; mechanical properties; rheology

INTRODUCTION

The use of natural-organic fillers in the production of polymer composites became popular especially during the last years and it is due to several positive issues, such as the low cost of natural-organic fillers (which often come from wastes), the reduction of specific weight and of health hazards for employees (in case of inhalation), the satisfying esthetic features, the reduced environmental impact. In this latter case, in particular, these materials allow obtaining a significant reduction in the use of non-renewable (typically, oil-based) resources throughout the entire life-cycle of the product.[1–6] These features allow making them strongly competitive if compared to the traditional, inorganic-mineral fillers.

Several recent articles investigated polymer composites filled with a number of different natural-organic fillers (i.e., particles and fibers coming from natural resources, typically from plants), such as wood, hemp, sisal, kenaf, jute, starch, etc.[7–14] However, the rising concerns regarding the disposal of plastic goods request biodegradability of the product or, alternatively, its compostability. Natural-organic fillers are fully biodegradable, but their biodegradability can be made fruitless by the presence of a non-biodegradable polymer. In this sense, a possibility to overcome this problem is to use biodegradable polymer as a matrix.

Biodegradable polymers include materials such as polyesters, polyester amides, polyvinyl alcohol, starch, and its derivatives, polylactic acid, poly hydroxyalcanoates, cellulose, etc.[15]

Several research articles report about composites made of biodegradable polymers and natural-organic fillers. Biodegradable matrices used include Mater-Bi,[16–25] polylactic acid,[26–30] poly(hydroxybutyrate-*co*-hydroxyvalerate),[31] polyvinyl alcohol,[32] polybutylene succinate.[33]

Mater-Bi composites showed increased elastic modulus and HDT than the neat polymer.[18,19,21,34] Processing temperature and speed were found to strongly influence the final properties of the composites.[22–25] However, these materials often show an increased sensitivity to environmental humidity, thus suggesting to avoid their use in applications where high moisture conditions exist.[20,35]

In this work, we investigate the influence of several processing techniques on the final properties (mechanical, rheological, morphological) of Mater-Bi/wood

Correspondence to: R. Scaffaro (scaffaro@dicpm.unipa.it).

flour composites, to find the most suitable processing conditions for these materials. The role of two wood flour size classes (coarse or fine) was also assessed.

EXPERIMENTAL

The Mater-Bi grade TF01 used in this work was kindly provided by Novamont (Novara, Italy) and belongs to the recent vegetable oil-derived Mater-Bi family. The composition of this multiphase, polycondensation matrix is proprietary. The melt flow index measured at 150°C was 46 g/10 min (5 kg load).

The wood flour used in this work was kindly supplied by LA.SO.LE. (Percoto, Italy). Two different size classes were used: a coarse one, indicated throughout the work as "SDC" (average particle diameter 350–500 μm, average $L/D \approx 3.9$) and a fine one, indicated throughout the work as "SDF" (average particle diameter 150–200 μm, average $L/D \approx 2.8$). Before processing, wood flour was always dried in a ventilated oven at 70°C for 10 h.

Preparation and processing

Neat polymer and 15% (w/w) wood flour composites were melt processed using different equipments.

Mixing was carried out in a Brabender (Duisburg, Germany) PLE330 batch mixer ($T = 140$°C, $n = 30$ rpm), as long as to achieve a constant torque.

Extrusion was performed both in a single-screw extruder (SSE) and in a co-rotating twin-screw extruder (TSE). In the single-screw extruder (Brabender, $D = 19$ mm, $L/D = 25$) the temperature profile adopted was from 70°C (at the hopper) to 115°C (at the die), the speed was set at 30 rpm. The SSE was equipped with a slot die and connected to a Collin (Ebersberg, Germany) CR72 calendering system. The residence time, calculated with a color tracer, was estimated in 3.7–4 min. In the co-rotating twin-screw extruder ($D = 19$ mm, $L/D = 35$) manufactured by OMC (Saronno, Italy), the temperature profile adopted was from 90°C (at the hopper) to 125°C (at the die), the speed was set at 100 rpm. The residence time, calculated with a color tracer, was estimated in 2.3–2.8 min. These materials were therefore pelletized using an Accrapak (Burtonwood, England) BM15 grinder. Part of the material coming from the co-rotating extruder was further processed by injection molding in a Sandretto (Grugliasco, Italy) μ30 press, operating at 140°C, with a pressure of 900 bar and a residence time of 3–4 min, estimated with a color tracer.

Characterization

Compression molded specimens were obtained preparing sheets by a Carver (Wabash, IN) laboratory press (140°C, 4 min) and directly cutting them off the plates (thickness 0.5–1.3 mm, width 10 mm, length 90 mm). The same compression molding technique was also used for the materials fed out the batch mixer, while the specimens of the materials prepared by single-screw extrusion were directly cut off the calendered films. Injection molded (prepared as described earlier) specimens (about 3 mm thick, 12 mm wide, 140 mm long) were used for characterization without further modifications.

Tensile tests, according to ASTM D882, were performed using an Instron (Norwood, MA) mod. 3365 universal machine on the compression molded and the injection molded specimens, with a 30 mm initial length. At least 10 replicates were tested and the average values were calculated. The reproducibility was fairly good (maximum data scattering was ±10% for the elastic modulus, ±15% for the tensile strength, ±20% for the elongation at break).

According to the procedure described in previous works,[35,36] the dispersion of the filler inside the composite was estimated by calculating the "mixing index":

$$\mathrm{MI} = 1 - \frac{s}{s_0} \tag{1}$$

where s is the square root of the actual variance

$$s^2 = \frac{1}{(N-1)} \sum_{i=1}^{N} (c_i - \bar{c})^2 \tag{2}$$

N is the number of measurements, c_i is the concentration of the ith observation, $\bar{c}$ is the mean concentration, s_0 the square root of the maximum variance.

The filler particles, extracted by using an appropriate solvent, were also used for evaluating the aspect ratios after processing. For this purpose, a Leica (Wetzlar, Germany) optical microscope was used to get micrographs of the fibers (not reported here) and the Leica QWin® software was used for the measurements.

Flow curves were measured by using a Rheometric Scientific (Piscataway, NJ) SR5 plate-plate rotational rheometer operating at 140°C.

To get further understanding of some phenomena emerged during the characterization, SEM analysis was carried out, using a Philips (Eindhoven, The Netherlands) ESEM XL30 apparatus on specimens broken in liquid nitrogen and covered with gold to make them conductive.

RESULTS AND DISCUSSION

The flow curves of neat and composite materials allowed observing three different features, namely, the effect of the processing, the effect of the presence of the wood flour, and the effect of the filler size.

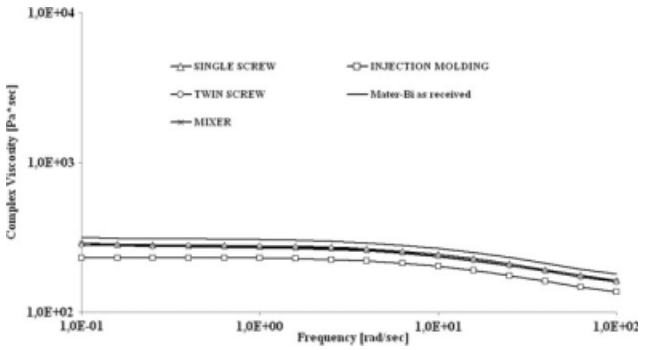

Figure 1 Flow curves of neat materials.

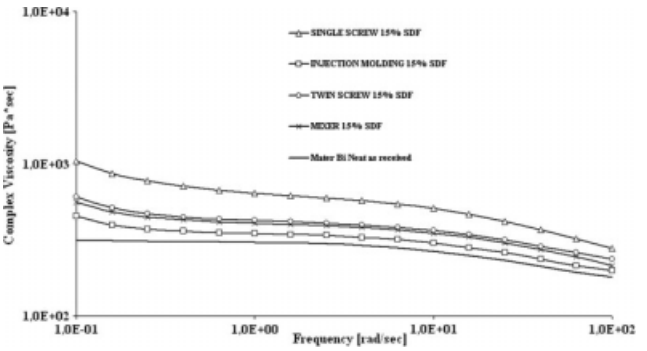

Figure 3 Flow curves of composite (SDF) materials.

For the unfilled polymer, Figure 1, the processing, comparing to the raw material, causes a decrease of the viscosity in the whole frequency range here investigated. In particular, the decrease is remarkable for the injection molded sample, while is less dramatic, although considerable, for the extruded and the mixed materials. This result can be interpreted considering that the thermomechanical stress acting on the melt during processing causes a partial breaking of the macromolecules. Reasonably, the two processing steps for the injection molded polymer imply a more remarkable degradation and, consequently, a lower viscosity. The same interpretation holds for the filled systems, Figure 2. Also in that case, in fact, the injection molded systems display viscosities lower than those observed for the extruded materials.

The flow curves of the neat materials show a Newtonian behavior only at relatively low shear rates while, on increasing the shear rate, also the non-Newtonian behavior increases.

The addition of the wood flour, Figure 2, leads to a significant increase of the viscosity of all the materials. As already observed and discussed about the neat materials, the flow curves of the injection molded systems are lower than those of the extruded materials. This is a further confirmation of the hypotheses regarding the polymer matrix degradation. Furthermore, the filled materials do not display a Newtonian plateau and, at low shear rates, the tendency to a yield stress is clearly visible. At higher shear rates, the flow curves approach each other. The explanation for this behavior can be given assuming that gel-like structures are present in the material at very low shear rates. These gel-like structures are due to the matrix-fiber interactions and exert a resistance to the flow which finds its macroscopic outcome in the appearance of a yield stress. When the shear rate increases, however, the gel-like structures are disrupted and the filled materials behave basically as a suspension of solid particles in a melt phase.[37–39]

As regards the effect of filler size, SDF filled materials seem to show, if compared to the SDC filled ones, a more important role of matrix-filler interactions, since the initial slopes (i.e., at the lowest shear rates) of their flow curves are steeper, Figure 3. However, on average, SDC filled materials show higher viscosities (at low and intermediate shear rates, i.e., in the typical range of the processing equipments here used), except for the injection molded materials, where the flow curves are almost coincident and the yield stress is less significant. Finally, the rheological measurements confirm that the viscosity of this material is controlled by the degradation of the matrix.

SEM micrographs of the neat materials are shown in Figure 4(a–d).

The observation of the fracture surfaces puts into evidence that the morphology of the mixer-processed material is relatively smooth and compact. In SSE material, on the other hand, small aggregates are visible, as well as the orientation lines due to the calendering operation. The structure of the TSE material shows also many small and evenly distributed aggregates, reasonably connected with a multiphasic nature of the matrix. The injection molded material shows a significantly smoother and compact internal morphology, due to the high pressure attained during this kind of process. The fact that the aggregates are observed mainly in the SSE and TSE samples may be due to the overall shorter processing times, in comparison to mixer and injection

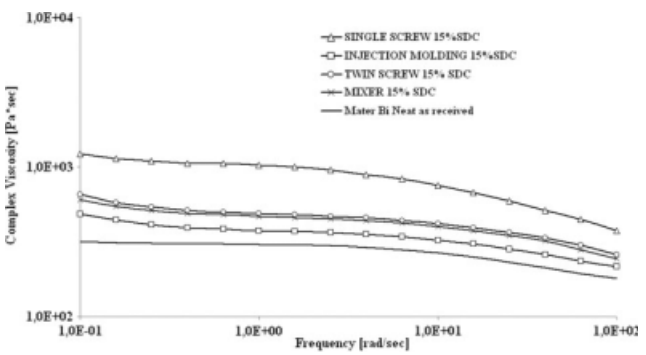

Figure 2 Flow curves of composite (SDC) materials.

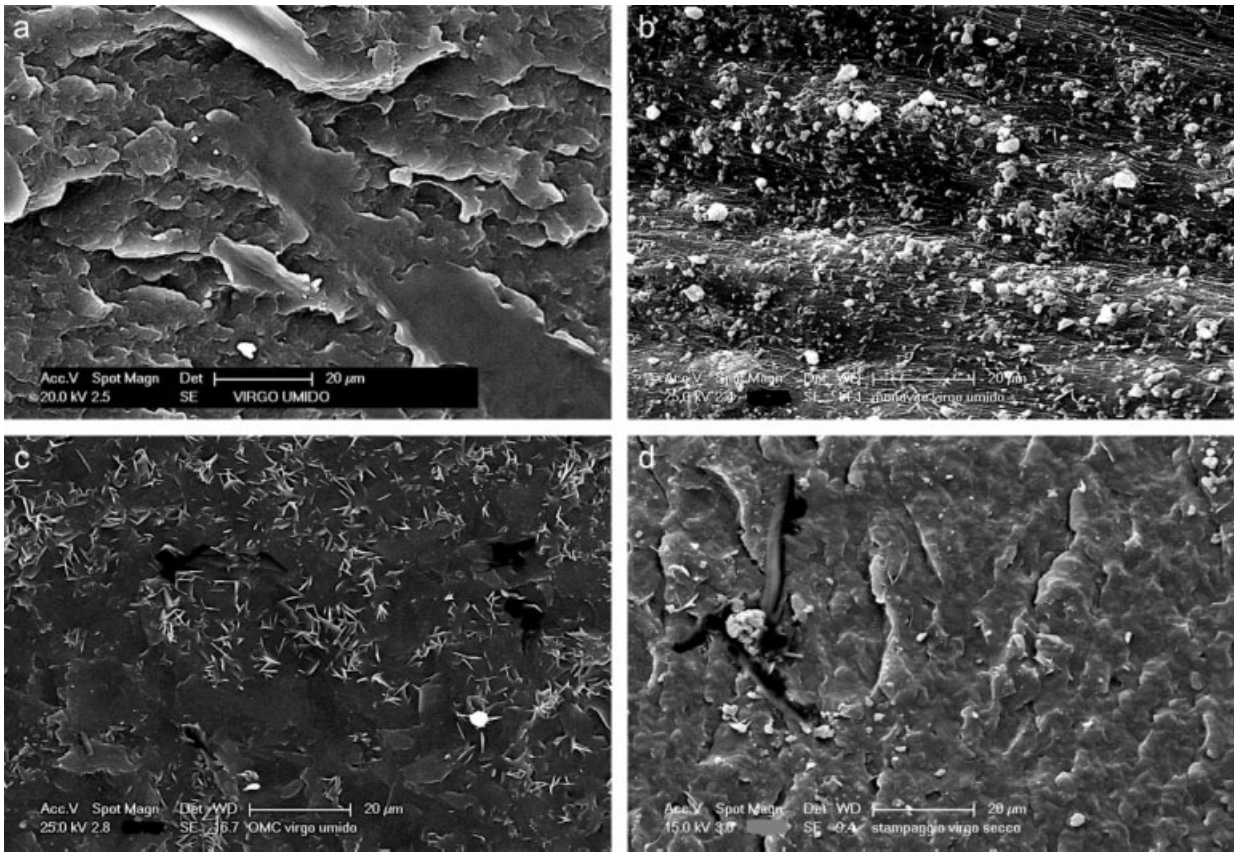

Figure 4 SEM micrographs of the morphologies of unfilled samples processed by batch mixer (a), single-screw extruder and calender (b), twin-screw extruder (c), and injection molding (d).

molding processed materials. In this latter case, no aggregates are visible in the SEM micrographs, at least at the same magnification scale.

Concerning with to the bulk morphologies of the composites, some representative SEM micrographs (SDF filled materials) are shown in Figure 5(a–d). The magnification is slightly lower than in the case of neat samples, to get a better overview of the morphology and the dispersion of the filler in the matrix.

The material prepared in the batch mixer seems to be compact. However, an isolated fiber is clearly visible, thus indicating that this processing technique did not allow obtaining a good fiber adherence. Significantly better morphologies are shown by the extruded and the injection molded materials. The fracture surface is significantly more compact and there is no evident fiber pull-out, indicating an improved polymer-filler adherence. This may be related to the higher packing achieved in those processing (especially in the injection molding).

The morphology of the composites is, of course, connected with their mechanical properties. The dimensionless elastic modulus for all the investigated materials is reported in Figure 6. The actual average values of the neat samples (E_0, measured in MPa) are reported in the bars of the corresponding material.

The addition of wood flour leads to a significant increase of the elastic modulus. The stiffness is similar for all the processing techniques, except for injection molding, where it is significantly lower both for the neat and the filled samples. This is probably due to the degradation phenomena affecting the matrix caused by the TSE/injection molding double processing, already discussed in the rheological part. No significant differences were measured between SDC and SDF composites.

The dimensionless tensile strength values are reported in Figure 7. The actual average values of neat samples (TS_0, measured in MPa) are reported in the bars of the corresponding materials.

The tensile strength of the mixer samples is relatively low, and this is probably due to the poor adherence between polymer matrix and fiber, as highlighted by SEM analysis as in Figure 5(a). The highest values of tensile strength were obtained by SSE and by injection molding. In the first case, this is probably due to the point that tensile tests were performed on samples cut off the extruded sheet in the longitudinal (machine) direction, where an orientation of the macromolecules occurs [as also shown

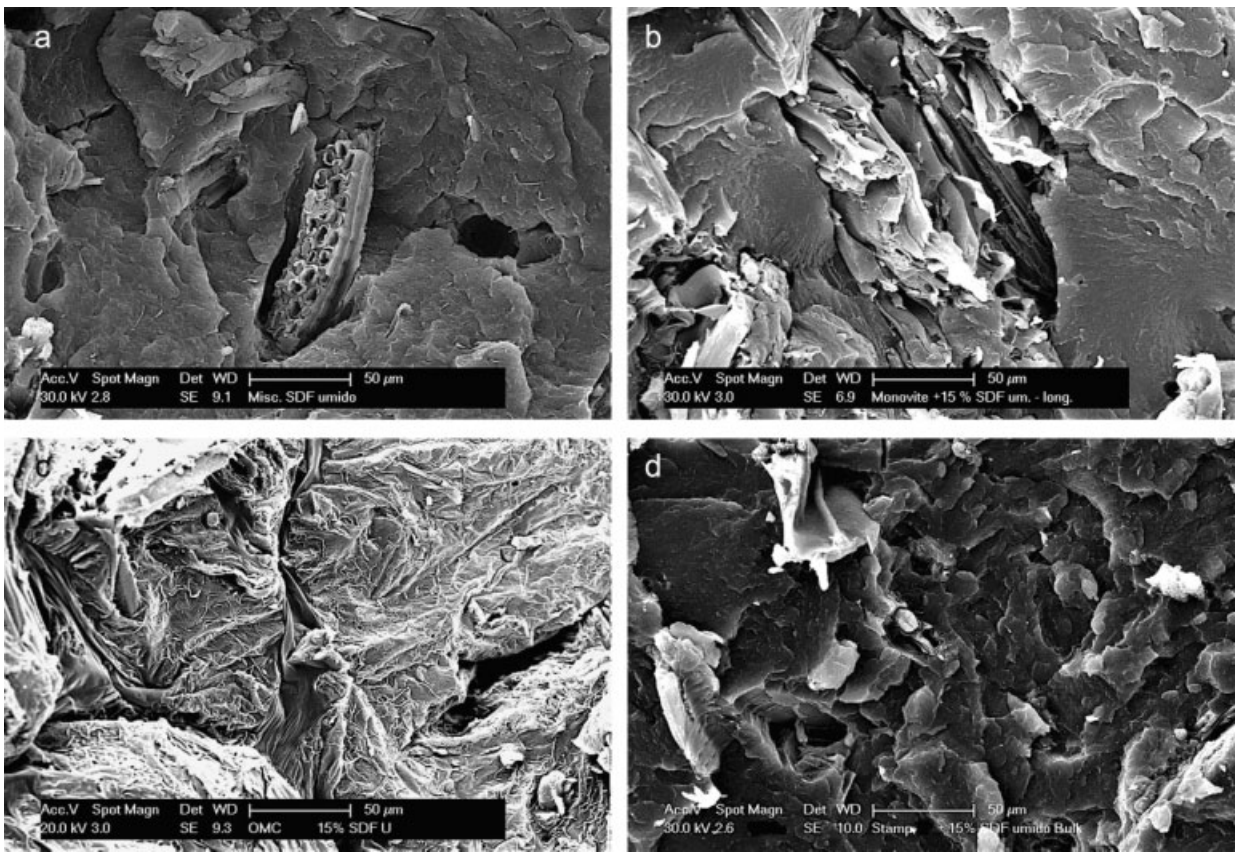

Figure 5 SEM micrographs of the morphologies of filled samples processed by batch mixer (a), single-screw extruder and calender (b), twin-screw extruder (c), and injection molding (d).

in Fig. 4(b)]. This feature is reasonably the cause of the improvement of the tensile strength. In the second case, the increase of tensile strength—especially interesting considering that this is the only processing technique which allows obtaining an improvement with respect to the neat polymer—is reasonably due to the compact morphology as shown in Figure 5(d).

Finally, elongation at break is reported in Figure 8.

The addition of wood flour, as expected,[34,35] leads to a dramatic decrease of the elongation at break. There are no significant differences between SDC and SDF composites, and the only remarkable result is the high deformability of neat twin-screw processed samples.

An interesting phenomenon was observed during the tensile tests, which also had a consequence on the measured values of the elongation at break. The neat specimens subjected to the tensile tests

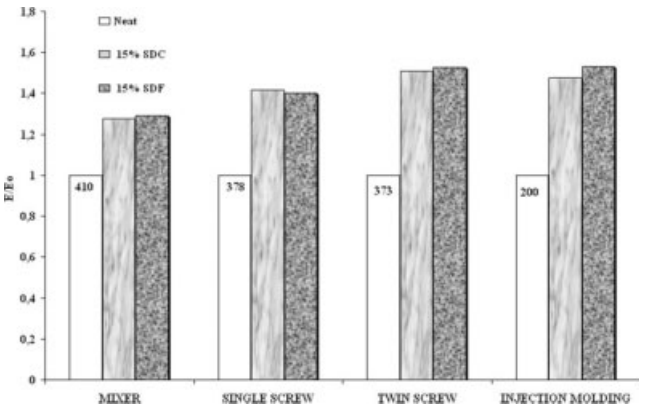

Figure 6 Dimensionless elastic modulus of neat and composite samples.

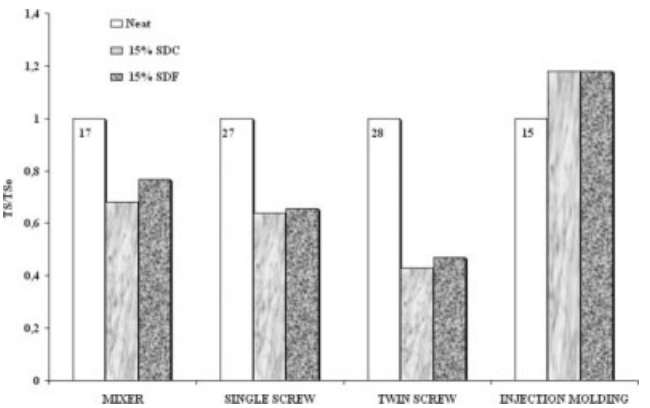

Figure 7 Dimensionless tensile strength of neat and composite samples.

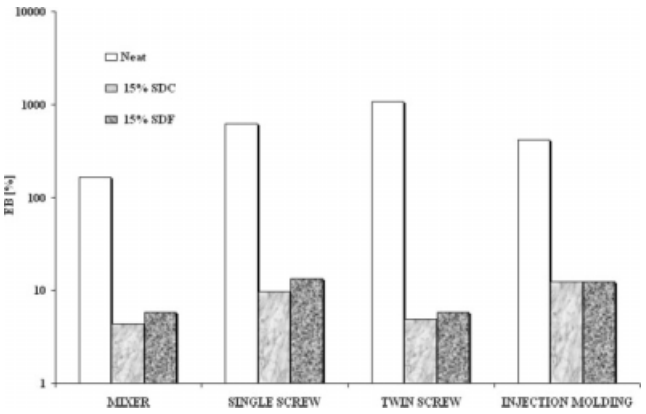

Figure 8 Elongation at break of neat and composite samples.

exhibited, during the deformation, significant swelling, and whitening effects in the elongated zone (i.e., the neck-in section), as shown in Figure 9(a–d).

It can be observed that the described phenomena occurred especially in the TSE, SSE, and injection molded samples. They could be hardly noticed in the simply mixed materials.

To find an explanation for this phenomenon, SEM analysis was carried out on the specimens coming out of the tensile tests, after fracturing the neck-in zone in liquid nitrogen. The micrographs are reported in Figure 10(a–d).

It can be observed that the morphology of the neck-in zone shows several clusters of small holes and cavities, which are likely to be the reason for the observed swelling and whitening phenomena, as well as the high values of elongation at break of the neat samples. Furthermore, the formation of these clusters seems to be reduced in the material coming from the mixer, which is at the same time the one that exhibited the lowest elongation at break. These clusters (and the resulting swelling and whitening phenomena) are probably the outcome of foaming-like phenomena. It is likely, in fact, that the reciprocal flowing of the macromolecular chains during the tensile deformation generates friction enough to induce a significant heat generation, and therefore, the creation of local temperature peaks. This may, in turn, induce the formation of the bubble clusters by foaming-like phenomena. Furthermore, it has been reported that, on increasing the temperature, the foaming processes in similar biodegradable polymer systems can occur to a greater extent.[40] Therefore, the actual peak temperature of the neck-in zone during the elongation

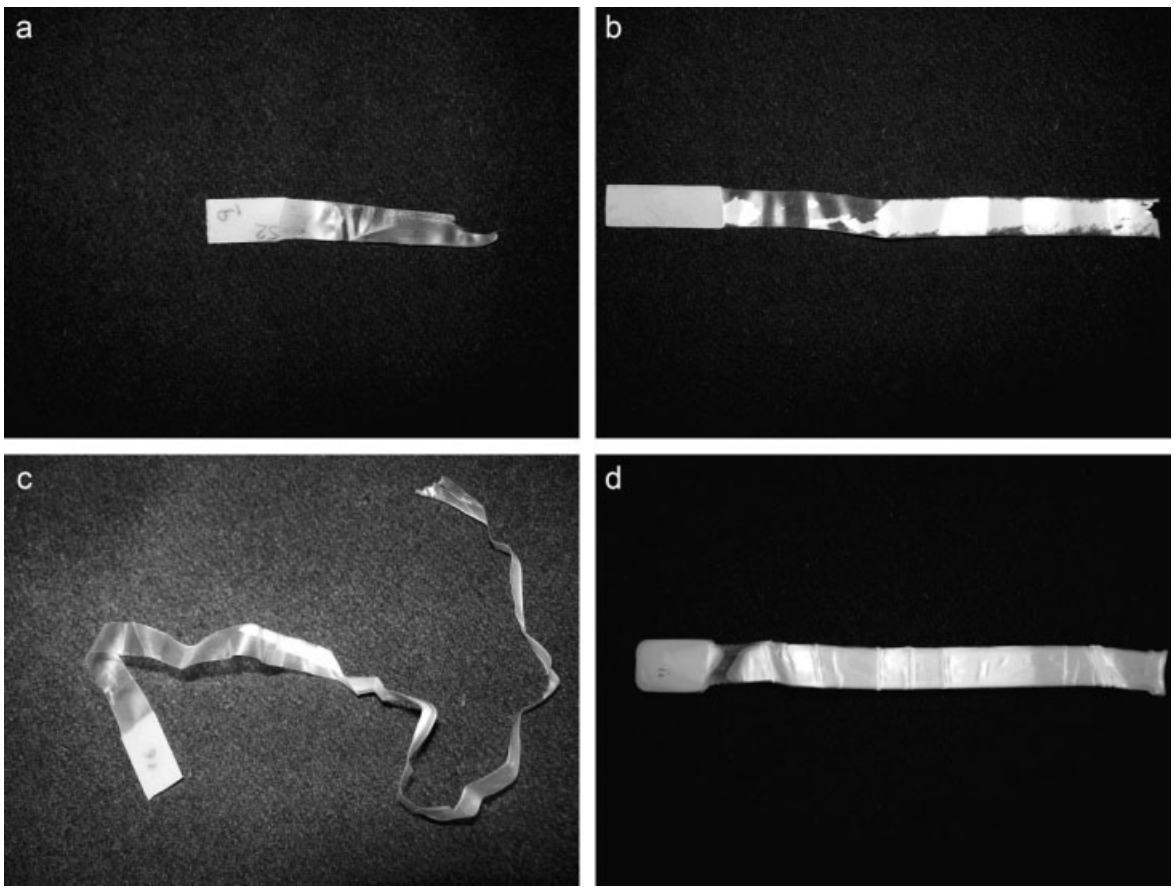

Figure 9 Neat samples, respectively, processed by batch mixer (a), single-screw extruder and calender (b), twin-screw extruder (c), and injection molding (d) after tensile deformation.

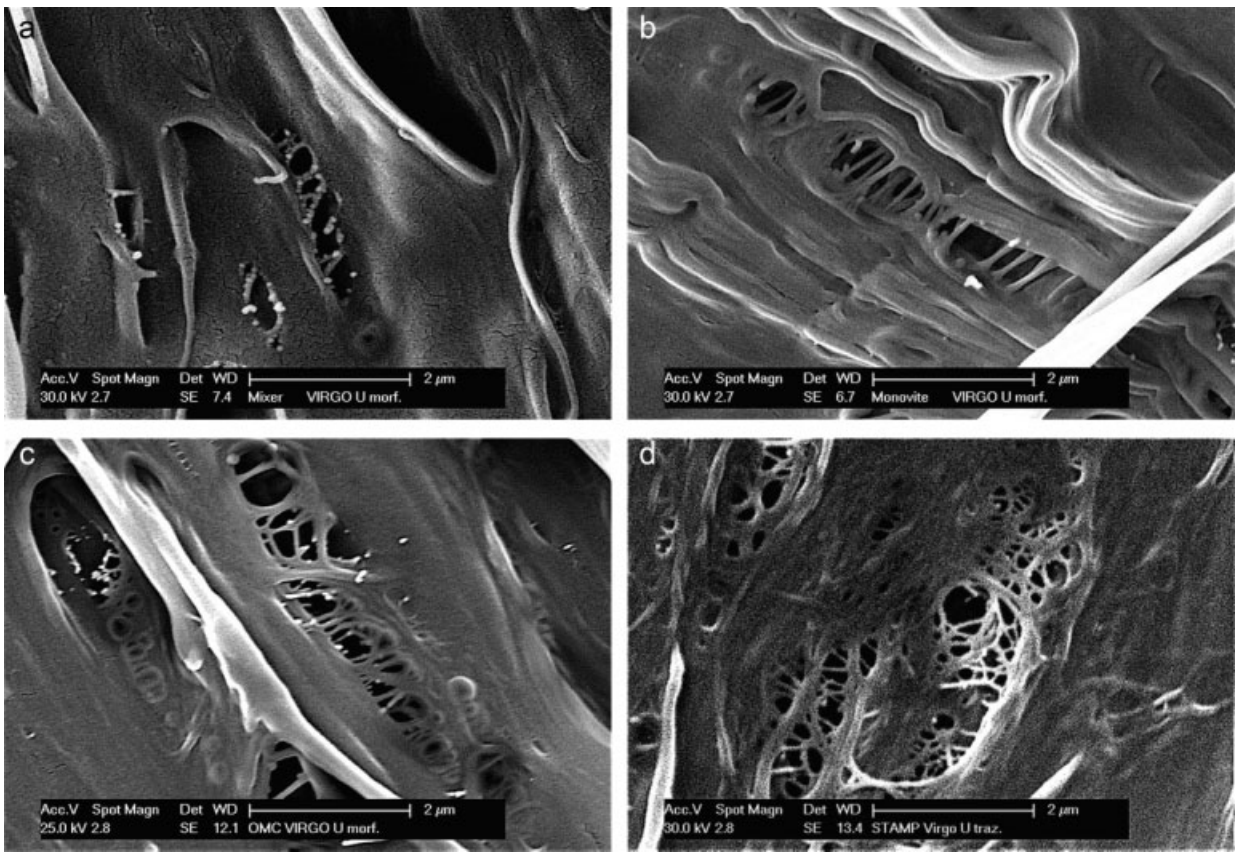

Figure 10 SEM micrographs of the internal morphologies of neat samples processed by batch mixer (a), single-screw extruder and calender (b), twin-screw extruder (c), and injection molding (d) after tensile deformation.

was measured using a Fluke (Everett, WA) Mod. 66 laser thermometer. The results (where ΔT = difference between actual specimen temperature and environment temperature) were averaged between at least five specimens and are shown in Table I.

The measurements confirm that there is a significant local temperature increase and this can be the cause of the foaming-like phenomena. The temperature increases are in agreement with the results of elongation at break: the highest in the TSE samples and the lowest in the mixer-processed ones. As a matter of fact, on increasing the temperature, a corresponding reduction of the tensile stress should be observed but this is not true for our systems. The explanation can be found considering that the foaming-like phenomenon did not affect the tensile strength to the same extent. As shown by representative stress–strain curves reported in Figure 11, significant strain-hardening occurred in the extruded samples, thus, the strain-hardening led to higher tensile strength values. Moreover, it is worth considering that the processed materials show a different behavior (refer also the rheological and the morphological analysis), therefore, the effect of the tensile stress cannot be predicted on the basis of the sole temperature increase.

Furthermore, the SEM observations showed a reduced bubble formation in the mixer-processed materials, while it was more evident in the TSE and the injection molding processed samples, and this is also in agreement with the above reported considerations. The foaming-like phenomena, which account for the unexpected values of elongation at break of some of the samples, were not observed in the filled materials. This is in agreement with the above explanations, since the presence of the filler strongly reduces the deformability of the material, and thus, the ability of the macromolecules to flow reciprocally under the tensile load. The reduced reciprocal flow, therefore, cannot generate enough heat to trigger the foaming: in this case, the local temperature increases were below 2–3°C. Therefore, the mechanical behavior is here controlled by the stiffening effect caused by the filler.

TABLE I
Local Temperature Increases of Specimens During Tensile Tests

	Mixer	Single screw	Twin screw	Injection molding
ΔT (°C)	9	21	24	18

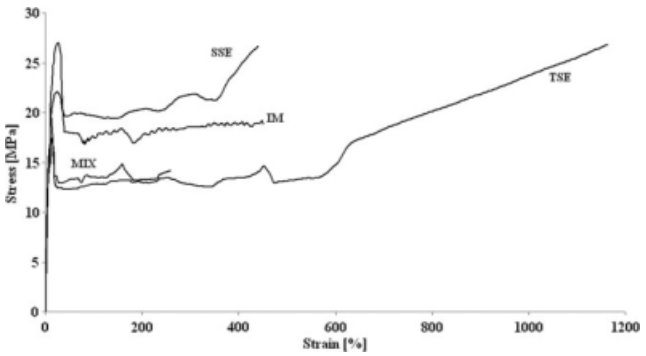

Figure 11 Stress/strain curves of neat samples.

In conclusion, the mechanical properties of these systems depend on many factors, which in turn depend on the morphology achieved during the melt processing steps: thermomechanical degradation, adherence between matrix and fibers, and during the tensile tests, i.e., foaming-like structure development and increase of the temperature. All these factors act in different ways and in some cases are in competition among them. As for the elastic modulus, despite the better bulk morphology, the injection molded samples showed the lowest value of the modulus, probably due to the degradation phenomena undergone during the double processing steps, as confirmed by the rheological data. On the other hand, the better morphology of these samples is the responsible of the remarkable increase of the elastic modulus with respect to the neat polymer.

As for the tensile strength, it has been observed that the relatively high values of SSE samples are probably due to the orientation of the macromolecules in the machine direction, while the increase of tensile strength in the injection molded composites is likely to be due to the good morphology achieved.

Finally, the differences between the mechanical properties of SDC and SDF composites, were, on the whole, small and lower than the expected based on the initial different *L/D* ratios of the fillers. There are two different factors to be taken into account.

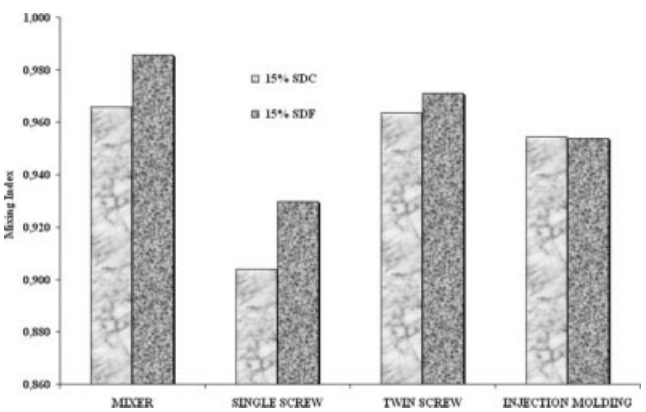

Figure 12 Mixing index of the SDC and SDF composites.

TABLE II
***L/D* Ratios of SDC and SDF Fibers Before and after Processing**

Sample	Before processing	Extracted from twin-screw processed samples	Extracted from injection molded samples
SDF	2.8 (±1.0)	2.8 (±0.6)	2.7 (±0.5)
SDC	3.9 (±1.2)	3.5 (±1.0)	3.2 (±0.8)

The first is related to the filler dispersion inside the polymer matrix. This can be estimated by using the "Mixing Index" (MI),[35,36] which is shown in Figure 12 for all the investigated composites.

The results of the tensile tests showed that, on average, SDF composites exhibited slightly higher resistance values than SDC composites. Mixing index provides a confirmation and a justification of this trend, since higher values of MI were found for the SDF composites, even if the differences are little. It is important to underline that the mixing index is just one of the variables influencing the mechanical properties, and therefore, it cannot be used as the only parameter to explain the mechanical performance of the composites, especially when the processing techniques are different. However, it can be effectively used to find an explanation for the different behavior upon changing the filler size, when the processing technique is the same.

The second factor—which can further and better explain the point that SDF and SDC tensile resistance values are very close each other—is related to the actual *L/D* ratios after processing. These are, in fact, the actual aspect ratios of the filler inside the composite material as in operative conditions. Some representative values are reported in Table II.

The data clearly indicate that, after processing, the gap in the aspect ratio between SDC and SDF is reduced to become practically not influent, as in the case of injection molding which, in fact, led to samples with almost identical mechanical properties, regardless of the different nominal filler size. The reduction of the aspect ratio is due to the mechanical stresses which arise during processing and that are more relevant when the aspect ratio of the fibers is higher.[41,42]

CONCLUSIONS

In this work, the processability and the influence of the processing techniques on the properties of Mater-Bi/wood flour composites were investigated. The results concerning rheological tests and flow curves showed that injection molding led to a partial degradation of the macromolecular chains, thus lowering the melt viscosity and the rigidity of the material. Differently, single-screw extrusion followed by calendering and twin-screw extrusion led to

relatively high modulus and viscosity. The addition of wood flour allowed obtaining a significant increase of the rigidity, with a reduction of the ductility; this was particularly true in the case of injection molded materials. The differences between the two different filler size classes were small and this was explained measuring that the aspect ratios of the two after processing became similar. The slightly higher resistance of SDF composites was explained considering a better dispersion of this filler.

An interesting foaming phenomenon was observed in all the unfilled samples, especially those processed in the twin-screw extruder, during the tensile tests, leading to a high deformability. This was attributed to local temperature increases due to the macromolecular chains friction.

The authors thank Novamont for supplying the material and for technical support. This work was financially supported by University of Palermo (Ex-60% Year 2005).

References

1. Joseph, P. V.; Joseph, K.; Thomas, S. Comp Sci Tech 1999, 59, 1625.
2. Gachter, R.; Muller, H. Plastics Additives, 3rd ed.; Hanser Publishers: New York, 1990.
3. Rozman, H. D.; Lai, C. Y.; Ismail, H.; Mohd Ishak, Z. A. Polym Int 2000, 49, 1273.
4. Canchè-Escamilla, G.; Rodriguez-Laviada, J.; Cauich-Cupul, J. I.; Mendizabal, E.; Puig, J. E.; Herrera-Franco, P. J. Comp Pt A 2002, 33, 539.
5. Coutinho, F. M. B.; Costa, T. H. S.; Carvalho, D. L. J Appl Polym Sci 1997, 65, 1227.
6. Joshi, S. V.; Drzal, L. T.; Mohanty, A. K.; Arora, S. Comp Pt A 2004, 35, 371.
7. Danjaji, I. D.; Nawang, R.; Ishiaku, U. S.; Ismail, H.; Mohd Ishak, Z. A. J Appl Polym Sci 2000, 79, 29.
8. Sharma, N.; Chang, L. P.; Chu, Y. L.; Ismail, H.; Mohd Ishak, Z. A. Polym Degrad Stab 2001, 71, 381.
9. La Mantia, F. P.; Tzankova Dintcheva, N.; Morreale, M.; Vaca-Garcia, C. Polym Int 2004, 53, 1888.
10. Raj, R. B.; Kokta, V. B.; Maldas, D.; Daneault, C. J Appl Polym Sci 1989, 37, 1089.
11. Balasuriya, P. W.; Ye, L.; Mai, Y. W.; Wu, J. J Appl Polym Sci 2002, 83, 2505.
12. Wool, R. P.; Raghavan, D.; Wagner, G. C.; Billieux, S. J Appl Polym Sci 2000, 77, 1643.
13. Nitz, H.; Semke, H.; Mulhaupt, R. J Appl Polym Sci 2001, 81, 1972.
14. Chen, H. L.; Porter, R. S. J Appl Polym Sci 1994, 54, 1781.
15. Mohanty, A. K.; Misra, M.; Hinrichsen, G. Macromol Mater Eng 2000, 276, 1.
16. Alvarez, V. A.; Ruseckaite, R. A.; Vazquez, A. Polym Degrad Stab 2006, 91, 3156.
17. Alvarez, V. A.; Vazquez, A. Polym Degrad Stab 2004, 84, 13.
18. Alvarez, V. A.; Vazquez, A.; Bernal, C. J Comp Mat 2006, 40, 21.
19. Alvarez, V. A.; Vazquez, A.; Bernal, C. Polym Compos 2005, 26, 316.
20. Alvarez, V. A.; Fraga, A. N.; Vazquez, A. J Appl Polym Sci 2004, 91, 4007.
21. Puglia, D.; Tomassucci, A.; Kenny, J. M. Polym Adv Technol 2003, 14, 749.
22. Alvarez, V.; Iannoni, A.; Kenny, J. M.; Vazquez, A. J Compos Mat 2005, 39, 2023.
23. Alvarez, V. A.; Terenzi, A.; Kenny, J. M.; Vazquez, A. Polym Eng Sci 2004, 44, 1907.
24. Johnson, M.; Tucker, N.; Barnes, S.; Kirwan, K. Ind Cro Prod 2005, 22, 175.
25. Johnson, R. M.; Tucker, N.; Barnes, S. Polym Test 2003, 22, 209.
26. Hwan Lee, S.; Wang, S. Comp Pt A 2006, 37, 80.
27. Huda, M. S.; Drzal, L. T.; Mohanty, A. K.; Misra, M. Comp Sci Tech 2008, 68, 424.
28. Bax, B.; Mussig, J. Comp Sci Tech 2008, 68, 1601.
29. Garcia, M.; Garmendia, I.; Garcia, J. J Appl Polym Sci 2008, 107, 2994.
30. Pilla, S.; Gong, S.; O'neill, E.; Rowell, R.; Krzysik, A. Polym Eng Sci 2008, 48, 578.
31. Keller, A. Comp Sci Tech 2003, 63, 1307.
32. Imam, S. H.; Cinelli, P.; Gordon, S. H.; Chiellini, E. J Polym Environ 2005, 13, 47.
33. Kim, H.-S.; Yang, H.-S.; Kim, H.-J. J Appl Polym Sci 2005, 97, 1513.
34. Morreale, M.; Scaffaro, R.; Maio, A.; La Mantia, F. P. Comp Pt A 2008, 39, 1537.
35. Morreale, M.; Scaffaro, R.; Maio, A.; La Mantia, F. P. Comp Pt A 2008, 39, 503.
36. Kalyon, D. M.; Lawal, A.; Yazici, R.; Yaras, P.; Railkar, S. Polym Eng Sci 1999, 39, 1139.
37. Ottani, S.; Valenza, A.; La Mantia, F. P. Rheol Acta 1988, 27, 172.
38. Kitano, T.; Kataoka, T.; Nagatsuka, Y. Rheol Acta 1984, 23, 408.
39. Suetsugu, Y.; White, J. L. J Appl Polym Sci 1983, 28, 1481.
40. Marrazzo, C.; Di Maio, E.; Iannace, S. J Cell Plast 2007, 43, 123.
41. La Mantia, F. P.; Morreale, M.; Mohd Ishak, Z. A. J Appl Polym Sci 2005, 96, 1906.
42. La Mantia, F. P.; Morreale, M. Polym Eng Sci 2006, 46, 1131.